

## ORIGINAL ARTICLE

# Semiphysiologically Based Pharmacokinetic Model for Midazolam and CYP3A Mediated Metabolite 1-OH-Midazolam in Morbidly Obese and Weight Loss Surgery Patients

MJE Brill<sup>1,2</sup>, PAJ Väitalo<sup>1</sup>, AS Darwich<sup>3</sup>, B van Ramshorst<sup>4</sup>, HPA van Dongen<sup>5</sup>, A Rostami-Hodjegan<sup>3</sup>, M Danhof<sup>1</sup> and CAJ Knibbe<sup>1,2\*</sup>

This study aimed to describe the pharmacokinetics of midazolam and its cytochrome P450 3A (CYP3A) mediated metabolite 1-OH-midazolam in morbidly obese patients receiving oral and i.v. midazolam before ( $n = 20$ ) and one year after weight loss surgery ( $n = 18$ ), thereby providing insight into the influence of weight loss surgery on CYP3A activity in the gut wall and liver. In a semiphysiologically based pharmacokinetic (semi-PBPK) model in which different blood flow scenarios were evaluated, intrinsic hepatic clearance of midazolam ( $CL_{int,H}$ ) was 2 (95% CI 1.40–1.64) times higher compared to morbidly obese patients before surgery ( $P < 0.01$ ). Midazolam gut wall clearance ( $CL_{int,G}$ ) was slightly lower in patients after surgery ( $P > 0.05$ ), with low values for both groups. The results of the semi-PBPK model suggest that, in patients after weight loss surgery, CYP3A hepatic metabolizing capacity seems to recover compared to morbidly obese patients, whereas CYP3A mediated  $CL_{int,G}$  was low for both populations and showed large interindividual variability.

*CPT Pharmacometrics Syst. Pharmacol.* (2016) 5, 20–30; doi:10.1002/psp4.12048; published online 18 December 2015.

## Study Highlights

WHAT IS THE CURRENT KNOWLEDGE ON THE TOPIC?  Midazolam systemic plasma clearance increases upon weight loss surgery, whereas midazolam oral bioavailability is unchanged. • WHAT QUESTION DID THIS STUDY ADDRESS?  How does weight loss surgery affect CYP3A activity in the gut wall and liver? • WHAT THIS STUDY ADDS TO OUR KNOWLEDGE  This study shows that intrinsic hepatic metabolism of midazolam into 1-OH midazolam (hepatic CYP3A activity) is 1.5 times increased in patients after weight loss surgery, whereas intrinsic metabolism of midazolam into 1-OH midazolam in the gut wall was low and highly variable in both patient groups. • HOW THIS MIGHT CHANGE CLINICAL PHARMACOLOGY AND THERAPEUTICS  Weight loss surgery substantially increases hepatic CYP3A activity and therefore may increase the plasma clearance of CYP3A-mediated drugs. However, extrapolations should be performed with caution, because it is unclear how hepatic blood flow and perfusion is affected after weight loss surgery.

Weight loss surgery or bariatric surgery is widely and increasingly applied to treat morbid obesity (body mass index  $> 40 \text{ kg/m}^2$ ).<sup>1–3</sup> This type of surgery may profoundly affect drug pharmacokinetics, as the procedure reduces the stomach to a small pouch and, in case of a Roux and Y-gastric bypass (RYGB), 75–150 cm of the initial part of the small intestines, including the duodenum, is bypassed.<sup>4,5</sup> In addition, patients lose on average 32% of their body weight within one year,<sup>6</sup> which may affect clearance and the distribution of drugs as well.<sup>7</sup>

Previously, we showed in a population pharmacokinetic (PK) analysis that plasma clearance (CL) of the cytochrome P450 3A (CYP3A) substrate midazolam is 1.7 times increased in patients after a weight loss procedure in comparison to morbidly obese patients, whereas oral bioavailability ( $F_{total}$ ) was unaltered.<sup>8</sup> Similar results have been reported before for RYGB patients in comparison with age, gender,

and body mass index-matched control patients.<sup>9</sup> Although it is well known that CYP3A resides both in the gut and in the liver, these analyses that use total oral bioavailability ( $F_{total}$ ) as parameter do not allow for a distinction between the contribution of presystemic gut and presystemic liver metabolism. More specifically, oral bioavailability ( $F_{total}$ ) may be deduced to its individual contributors, which are the fraction absorbed ( $F_a$ ), the fraction escaping gut wall metabolism ( $F_G$ ), and the fraction escaping first pass hepatic metabolism ( $F_H$ ). As midazolam is a highly soluble and permeable drug,  $F_a$  is assumed to be equal to one in morbidly obese patients before and after surgery.<sup>10,11</sup> Keeping in mind the reported increase in midazolam systemic plasma clearance after a weight loss surgery,<sup>9,12</sup>  $F_H$  is expected to decrease after weight loss surgery. So, given the unchanged total bioavailability ( $F_{total}$ ) identified in these patients,<sup>8</sup> it may be hypothesized that the midazolam fraction escaping gut wall ( $F_G$ )

<sup>1</sup>Division of Pharmacology, Leiden Academic Centre for Drug Research, Leiden University, Leiden, The Netherlands; <sup>2</sup>Department of Clinical Pharmacy, St. Antonius Hospital, Nieuwegein, The Netherlands; <sup>3</sup>Manchester Pharmacy School, University of Manchester, Manchester, Great Britain, United Kingdom; <sup>4</sup>Department of Surgery, St. Antonius Hospital, Nieuwegein, The Netherlands; <sup>5</sup>Department of Anaesthesiology, Intensive Care, and Pain Management, St. Antonius Hospital, Nieuwegein, The Netherlands. \*Correspondence: CAJ Knibbe (c.knibbe@antoniusziekenhuis.nl)

Received 8 September 2015; accepted 4 November 2015; published online on 18 December 2015. doi:10.1002/psp4.12048

increases one year after weight loss surgery (see **Supplementary Information S1**). In theory, such an increase in  $F_G$  upon weight loss surgery may be attributed to the 75–150 cm bypass of the small intestine during an RYGB surgery<sup>4</sup> potentially causing reduced (intrinsic) CYP3A clearance in the gut.

Knowledge on the exact influence of a weight loss surgery on hepatic and gut wall CYP3A clearance is important because ~30% of all clinically used drugs are metabolized via this enzyme.<sup>12</sup> To fully characterize the influence of weight loss surgery on CYP3A-mediated drug metabolism in both the gut wall and the liver, a semiphysiologically based pharmacokinetic (semi-PBPK) model taking into account these distinct processes needs to be applied to both midazolam and the CYP3A-mediated metabolite 1-OH-midazolam concentrations obtained after oral and i.v. administration in these populations.<sup>13,14</sup> Such a semi-PBPK model consists of a compartment representing the gut wall, the portal vein, and the liver, and an empirical compartment model for midazolam and 1-OH-midazolam, representing the rest of the body. The model is parameterized on the basis of intrinsic clearance ( $CL_{int}$ ) for both the gut and the liver, blood flow, and fraction unbound in the blood or gut wall. In this model, intrinsic midazolam clearance in the liver or gut wall represents the capacity of the liver or gut wall to metabolize midazolam into 1-OH-midazolam and therefore represents CYP3A activity in these respective organs.

In this study, we aimed to describe both midazolam and its CYP3A-mediated metabolite 1-OH-midazolam in morbidly obese patients before and one year after weight loss surgery after both oral and i.v. administration using a semi-PBPK model, ultimately to evaluate how the intrinsic CYP3A activity in the gut wall and liver are affected by weight loss surgery and (loss of) body weight. In addition, the results are used to explore to what extent these results may affect other CYP3A substrates used after weight loss surgery.

## METHODS

### Study design and patients

In this study, data are used from a prospective observational cohort study in 20 morbidly obese patients at the day of laparoscopic weight loss surgery of whom 18 patients were studied again one year later (NTC01519726, EudraCT 2011-003293-93). Study design and characteristics have been described before and are repeated briefly below.<sup>8</sup>

In the study, morbidly obese patients undergoing a laparoscopic gastric bypass or sleeve surgery were eligible for inclusion. Patients were excluded if they used CYP3A-inducing or inhibiting medication,<sup>15</sup> used products containing grapefruit, wild grape, banpeiyu, pomegranate, star fruit, or blackberry within two weeks before the study, were pregnant, were breastfeeding, or suffered from renal insufficiency (epidermal growth factor receptor modification of diet in renal disease-4 <60 mL/min). Before participation, all patients gave written informed consent. One year after the weight loss procedure, 18 of the 20 patients were restudied using the same study design. At both occasions, patients received 7.5 mg oral and 5 mg i.v. midazolam separated by  $160 \pm 48$  minutes. Per

patient and occasion, a mean of 22 blood samples were collected to measure both midazolam and 1-OH midazolam concentrations. Plasma concentrations were measured using a method described before.<sup>16</sup> For 1-OH midazolam, the lower limit of quantification was 0.9 ng/mL and intra-assay and inter-assay coefficients of variation were 6.3% and 4.5%.

The study was approved by the local human research and ethics committee (NL35861.100.11) and was conducted according to the principles of the Declaration of Helsinki (version 22-10-2008) and in accordance with the Medical Research Involving Human Subjects Act (WMO) of the Netherlands.

### Population pharmacokinetic modeling

Population PK modeling was performed using NONMEM 7.3,<sup>17</sup> ADVAN 6 (PsN version 3.6.2), Pirana (version 2.9.0), and R (version 3.1.2) to visualize the data. Different structural models were tested to fit the midazolam and 1-OH-midazolam data from morbidly obese patients before and after weight loss surgery.

First, a regular population PK model was applied with a two-compartment model for 1-OH-midazolam, a three-compartment model for midazolam, and a transit compartment model for midazolam oral absorption in which the oral absorption rate ( $K_a$ ) was set equal to the transit compartment rate ( $K_{tr}$ ; intermediate model, **Figure 1a**). This model was based on earlier work on the PKs of midazolam not involving the 1-OH-midazolam metabolite.<sup>8</sup>

Second, a semi-PBPK model was applied to describe the data (semi-PBPK model, **Figure 1b**). The structural semi-PBPK model was adopted from Yang *et al.*<sup>13</sup> (2003) and Frechen *et al.*<sup>14</sup> (2013) and consisted of a compartment representing the gut wall, the portal vein, and the liver, and an empirical compartment model for midazolam and 1-OH midazolam, representing the rest of the body. In order to reduce runtimes, midazolam and 1-OH-midazolam were assumed to reach an instant equilibrium in the gut wall, portal vein, and liver compartment, which resulted in a simplified semi-PBPK model (see **Supplemental Information S2**). For midazolam, a three-compartment model was used and for midazolam oral absorption a transit compartment model in which the oral absorption rate was equalized to the transit compartment rate ( $K_{tr}$ )<sup>18</sup> was used. For 1-OH-midazolam, a two-compartment model was applied.

In the semi-PBPK model, hepatic ( $E_H$ ) and gut wall extraction ( $E_G$ ) of midazolam were defined as the input for the liver and gut wall compartment of the 1-OH-midazolam model, respectively. Hepatic extraction of midazolam ( $E_H$ ) and 1-OH-midazolam ( $E_{H,1-OH}$ ) was defined by the well-stirred model:

$$E_H = \frac{CL_{int,H} \cdot fu_B}{Q_{H,B} + (CL_{int,H} \cdot fu_B)} \quad (1)$$

where  $CL_{int,H}$  is the intrinsic hepatic clearance based on unbound blood concentrations,  $fu_B$  is the unbound concentration in blood, and  $Q_{H,B}$  is the hepatic blood flow.

The fraction escaping hepatic metabolism ( $F_H$ ) was defined as:

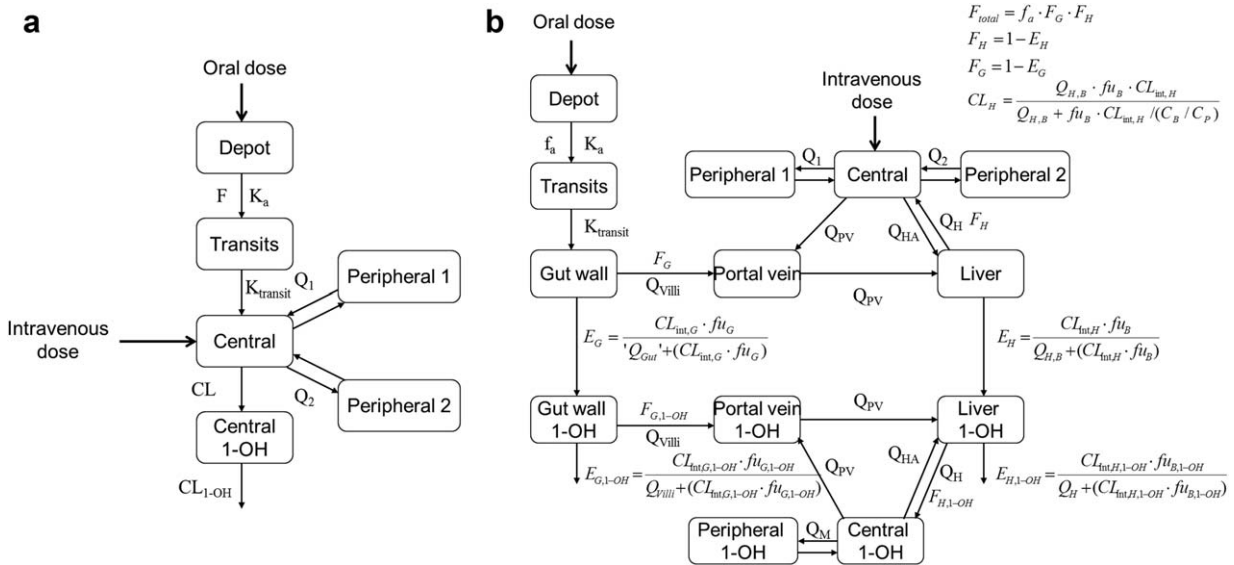


**Figure 1** Schematic representation of the intermediate population pharmacokinetic model (a) and semi-PBPK model (b) for midazolam and its 1-OH-midazolam metabolite (1-OH). B, blood;  $CL_{int}$ , intrinsic clearance; E, extraction ratio; G, gut wall;  $F_a$ , fraction absorbed into the gut wall;  $f_u$ , fraction unbound; H, hepatic;  $K_a$ , oral absorption rate;  $K_{transits}$ , transit compartment rate; Q is blood flow ( $Q_{villi}$ ,  $Q_{PV}$ ,  $Q_{HA}$ ,  $Q_H$ ) or intercompartmental clearance ( $Q_1$  and  $Q_2$ ); PV, portal vein.

$$F_H = 1 - E_H \quad (2)$$

For gut wall midazolam metabolism into 1-OH-midazolam ( $E_G$ ) the  $Q_{Gut}$  model was used<sup>19</sup>:

$$E_G = \frac{CL_{int,G} \cdot fu_G}{Q_{Gut} + (CL_{int,G} \cdot fu_G)} \quad (3)$$

where  $CL_{int,G}$  is the intrinsic gut wall clearance based on unbound blood concentrations,  $fu_G$  is the unbound drug concentration in the gut wall, and  $Q_{Gut}$  is defined by<sup>19</sup>:

$$Q_{Gut} = \frac{Q_{villi} \cdot CL_{perm}}{Q_{villi} + CL_{perm}} \quad (4)$$

where  $Q_{villi}$  is the villous blood flow and  $CL_{perm}$  is a term defining the permeability of the drug through the enterocytes in the gut wall. The fraction escaping gut wall metabolism was defined as:

$$F_G = 1 - E_G \quad (5)$$

Gut wall extraction of 1-OH-midazolam ( $E_{G,1-OH}$ ) was defined by:

$$E_{G,1-OH} = \frac{CL_{int,G,1-OH} \cdot fu_{G,1-OH}}{Q_{villi} + (CL_{int,G,1-OH} \cdot fu_{G,1-OH})} \quad (6)$$

Systemic plasma clearance ( $CL_H$ ) was derived from the hepatic midazolam intrinsic clearance and hepatic blood flow using<sup>20</sup>:

$$CL_H = \frac{Q_{H,B} \cdot fu_B \cdot CL_{int,H}}{Q_{H,B} + fu_B \cdot CL_{int,H} / (C_B / C_P)} \quad (7)$$

In which  $C_B / C_P$  is the blood to plasma ratio.

Values used for the drug parameters are listed in **Table 1**. The fraction of midazolam absorbed ( $F_a$ ) was fixed to one and it was assumed that no protein binding occurred in the gut wall (**Table 1**). As midazolam is an intermediate extraction ratio drug ( $E_H = \sim 0.4^{21-23}$ ), for the hepatic blood flow ( $Q_H$ ) three different scenarios were explored, including  $Q_H$  based on allometric scaling (scenario 1),<sup>24</sup>  $Q_H$  based on a model for cardiac output in obese and morbidly obese patients (scenario 2),<sup>25,26</sup> and a  $Q_H$  that was the same before and after weight loss surgery (scenario 3), see **Table 1**.

Discrimination between different structural models was made by comparison of the objective function value (OFV; i.e.,  $-2 \log$  likelihood). A  $P$  value  $< 0.05$ , representing a decrease of 3.84 in the OFV between nested models for one degree of freedom, was considered statistically significant. In addition, goodness-of-fit plots (observed vs. individual-predicted concentrations, observed vs. population-predicted concentrations, conditional weighted residuals vs. time, and conditional weighted residuals vs. population-predicted concentrations plots) of midazolam and 1-OH-midazolam were used for diagnostic purposes. Furthermore, the confidence interval (CI) of the parameter estimates, the correlation matrix, and visual improvement of the individual plots were used to evaluate the models. The internal validity of the population PK model was assessed by the bootstrap resampling method using 500 replicates.

For the statistical model, the individual parameter estimate (empirical Bayes estimate or *post hoc* value) of the  $i$ th individual was modeled according to:

$$\theta_i = \theta_{mean} \times e^{\eta_i} \quad (8)$$

where  $\theta_{mean}$  is the population mean, and  $\eta_i$  is a random variable for the  $i$ th individual with a mean of zero and variance of  $\omega^2$ , assuming log-normal distribution in the population. For residual

**Table 1** Values used for drug parameters and for three hepatic blood flow scenarios used in the semi-PBPK model

Parameter (unit) Reference	Scenario 1 Allometric scaling of the hepatic blood flow <sup>24</sup>	Scenario 2 Hepatic blood flow as a fraction of cardiac output <sup>25,26</sup>	Scenario 3 One hepatic blood flow for all individuals
Midazolam			
$f_a$		1 <sup>22</sup>	
B:P		0.66 <sup>22,41</sup>	
$f_{uG}$		1	
$f_{uB}$		0.0303 <sup>41</sup>	
$CL_{perm}$ (L/min)		0.177 <sup>19</sup>	
1-OH-midazolam			
B:P		1	
$f_{uG, 1-OH}$		1 <sup>19</sup>	
$f_{uB, 1-OH}$		0.106 <sup>42</sup>	
$CL_{perm}$		1	
Blood flows			
Cardiac output (L/min)	-	(9119- EXP (9.164 + -2.9 *10 <sup>-2</sup> * TBW + 3.91 *10 <sup>-4</sup> * TBW <sup>2</sup> + -1.91 *10 <sup>-6</sup> * TBW <sup>3</sup> )/1000	7
$Q_{hepatic}$ (L/min)	3.75 * TBW <sup>0.75</sup>	0.25 * CO <sup>26</sup>	0.25 * CO <sup>26</sup>
$Q_{hepatic}$ artery	0.25 * $Q_{hepatic}$ <sup>26</sup>	0.25 * $Q_{hepatic}$ <sup>26</sup>	0.25 * $Q_{hepatic}$ <sup>26</sup>
$Q_{portal}$ vein	0.75 * $Q_{hepatic}$ <sup>26</sup>	0.75 * $Q_{hepatic}$ <sup>26</sup>	0.75 * $Q_{hepatic}$ <sup>26</sup>
$Q_{small}$ intestine	0.4 * $Q_{hepatic}$ <sup>26</sup>	0.1 * CO <sup>19,26</sup>	0.4 * $Q_{hepatic}$ <sup>26</sup>
$Q_{mucosal}$	0.80 * $Q_{small}$ intestine <sup>19</sup>	0.80 * $Q_{small}$ intestine <sup>19</sup>	0.80 * $Q_{small}$ intestine <sup>19</sup>
$Q_{villi}$	0.60 * $Q_{mucosal}$ <sup>19</sup>	0.60 * $Q_{mucosal}$ <sup>19</sup>	0.60 * $Q_{mucosal}$ <sup>19</sup>

B:P, blood to plasma ratio;  $f_a$ , fraction absorbed in the gut wall;  $f_{ub}$ , fraction unbound in blood;  $f_{uG}$ , fraction unbound in gut wall;  $CL_{perm}$ , parameter representing the permeability through the enterocyte;  $Q$ , blood flow. The parameter values for midazolam and 1-OH-midazolam apply to all three scenarios.

variability, resulting from assay errors, model misspecifications and other unexplained sources, a proportional error model was used. The  $j$ th observed midazolam concentration of the  $i$ th individual ( $Y_{ij}$ ) is described by:

$$Y_{ij} = C_{pred,ij} \times (1 + \varepsilon_{ij}) \quad (9)$$

where  $C_{pred,ij}$  is the individual predicted midazolam concentration of the  $i$ th individual at the  $j$ th time, and  $\varepsilon_{ij}$  is a random variable with a mean of zero and variance of  $\sigma^2$ .

Data below the limit of quantification of the bioanalysis assay were provided by the laboratory and included in the dataset. Data below the limit of detection, defined as 30% of the lower limit of quantification, were deleted from the data set (5.7% for midazolam and 8.9% for 1-OH-midazolam).<sup>27</sup>

Based on our earlier PK analysis for midazolam, body weight on midazolam central, and peripheral volume of distribution for morbidly obese patients, and a separate parameter estimate for midazolam oral absorption rate and intercompartmental clearance in morbidly obese and weight loss patients were included in the model.<sup>8</sup> After inclusion of these midazolam covariates, a single covariate, the influence of weight loss surgery, was tested on midazolam gut wall and hepatic intrinsic clearance ( $CL_{int}$ ). The binary covariate before/after weight loss surgery was plotted independently against the individual *post hoc* values and eta estimates of midazolam intrinsic clearance estimates to visualize potential relations. The covariate "before/after weight loss surgery" was tested by means of a separate parameter or using the following equation:

$$P_i = P_p \times Z^{COV} \quad (10)$$

where  $P_i$  and  $P_p$  represent individual and population parameter estimate,  $Z$  the estimated factor of increase or decrease for the patients subgroup with COV equaling one.

The covariate was separately entered onto  $CL_{int,G}$  or  $CL_{int,H}$  and statistically tested ( $P < 0.05$ ) by use of the OFV and, if applicable, the 95% CI of the additional parameter. In addition, if applicable, it was evaluated whether the interindividual variability (eta) in the parameter concerned decreased upon inclusion of the covariate on the parameter and whether the trend in the eta vs. covariate plot had resolved.

### SimCYP simulations

The influence of weight loss surgery on mean systemic plasma clearance values of other CYP3A substrates was evaluated using the morbidly obese population in the SimCYP software and manipulation of the value for CYP3A hepatic abundance.<sup>28,29</sup> For each CYP3A-mediated drug, 10 trials of 10 individuals were simulated.

## RESULTS

The demographic data of the patients included in this analysis are provided in **Table 2**. **Figure 2a** shows the goodness-of-fit plots of the midazolam and 1-OH-midazolam plasma concentrations of both morbidly obese and weight loss patients on the basis of the regular population PK model, as shown in **Figure 1a** (intermediate model). These goodness-of-fit plots show that after the oral dose, midazolam concentrations were

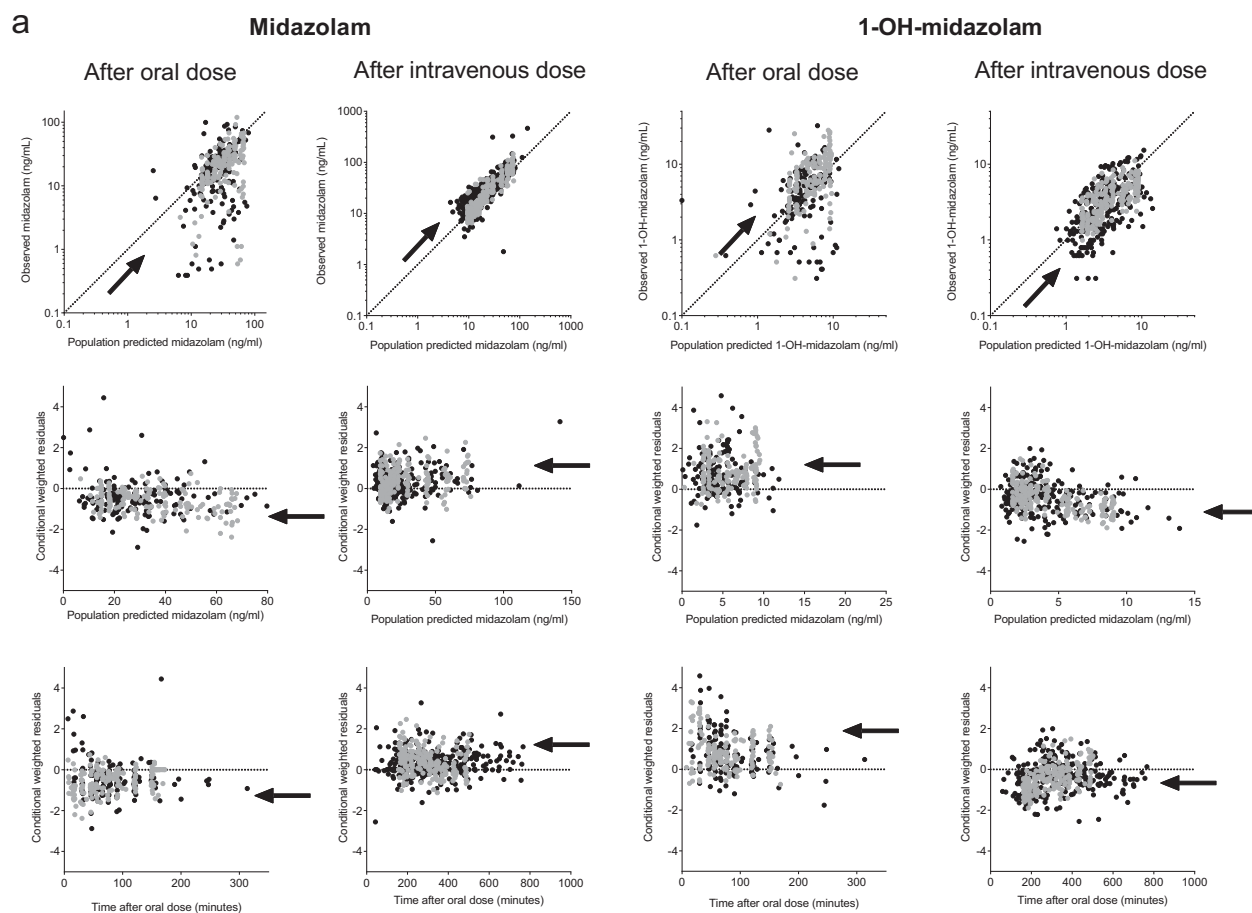


**Figure 2 (a)** Goodness-of-fit plots for midazolam (left) and 1-OH-midazolam (right) plasma concentrations for the population PK model (intermediate model, **Figure 1a**) for morbidly obese (black dots) and weight loss surgery patients (gray dots), including population predicted vs. observed plots (upper row), population predicted concentrations vs. conditional weighted residuals (middle row), and time after oral dose vs. conditional weighted residuals (lower row).

over-predicted, whereas midazolam concentrations after the i.v. dose were underpredicted (**Figure 2a**). In contrast, 1-OH-midazolam concentrations after oral dose were underpredicted by the model, whereas 1-OH-midazolam concentrations after i.v. dose were overpredicted. Furthermore, all of the conditional weighted residuals (CWRES) values stratified by patient group (obese or bariatric), administration type (oral or i.v.), and compound (parent or metabolite) were significantly different from zero ( $P < 0.001$  each) for the intermediate population PK model. The obvious misspecification of midazolam and its 1-OH-midazolam metabolite concentrations indicate the presence of substantial presystemic 1-OH-midazolam formation after oral administration and therefore, as a second step, a semi-PBPK model, including both presystemic midazolam metabolism at gut wall and hepatic level, was applied (**Figure 1b** and **Supplementary Information S3**). Application of the semi-PBPK model enabled a substantially improved prediction of midazolam and 1-OH-midazolam concentrations after both oral and i.v. dose and led to stratified CWRES mean values much closer to zero (**Figure 2b**).

Upon these findings, the semi-PBPK model was further explored for covariates, taking into account the different  $Q_H$  scenarios for obesity (see Methods and **Table 3**). The influ-

ence of weight loss surgery on midazolam intrinsic gut wall ( $CL_{int,G}$ ) and hepatic clearance ( $CL_{int,H}$ ) was evaluated by visual inspection of eta vs. covariate plots. **Figure 3** shows a trend of higher  $CL_{int,H}$  and slightly lower  $CL_{int,G}$  in weight loss patients in comparison to morbidly obese patients (**Figure 3**, upper panels). A separate parameter estimate for  $CL_{int,H}$  for morbidly obese and weight loss patients showed a 1.52 (with a 95% CI of 1.40–1.64) times higher intrinsic hepatic clearance in weight loss patients ( $-7 \Delta OFV$ ,  $P < 0.01$  for all  $Q_H$  scenarios) and a small decrease in interindividual variability (53% relative standard error of 19% vs. 48% (19%) for scenario 1). A separate parameter estimate for midazolam gut wall intrinsic clearance ( $CL_{int,G}$ ) did not significantly improve the model ( $-2 \Delta OFV$ ,  $P > 0.05$  for all  $Q_H$  scenarios). The two highest individual estimates for  $CL_{int,G}$  (see **Figure 3**, lower row, right plot) are two morbidly obese individuals for which the duration in between oral and i.v. midazolam dose was only 43 and 50 minutes as compared to a mean of  $171 \pm 57$  minutes for the other 18 morbidly obese patients. In addition, it seems that also these two individuals substantially contributed to the uncertainty of the parameter for intrinsic gut wall clearance of 1-OH-midazolam ( $CL_{int,G, 1-OH}$ ). Upon exclusion of these two

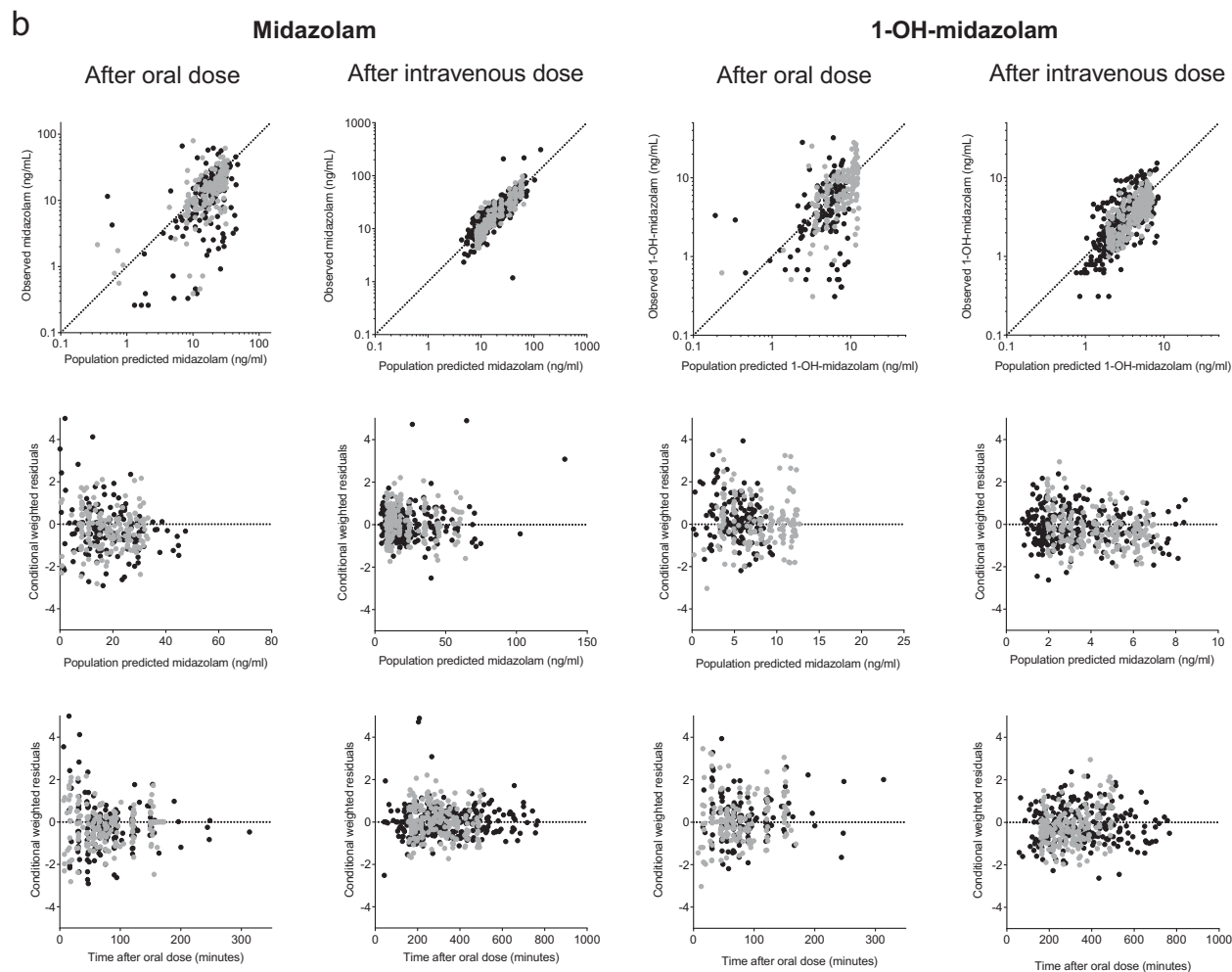


**Figure 2** (Continued). The arrows indicate the direction of model misspecification (**b**) goodness-of-fit plots for midazolam (left) and 1-OH-midazolam (right) blood concentrations for the final semi-PBPK model (**Figure 1b**) for morbidly obese (black dots) and weight loss patients (gray dots), including population predicted vs. observed plots (upper row), population predicted concentrations vs. conditional weighted residuals (middle row), and time after oral dose vs. conditional weighted residuals (lower row).

individuals, the parameter estimate for  $CL_{int,G 1-OH}$  changes from 11.9 L/min (relative standard error of 180%) to 6.7 L/min (relative standard error of 40%). However, exclusion of the two individuals resulted in the same final covariate model, and therefore for the final model all individuals were kept in the data.

Overall, the different  $Q_H$  scenarios (see Methods) resulted in slightly different hepatic intrinsic clearance estimates: 16.9 L/min (13%), 17.1 L/min (13%), and 12.6 L/min (16%) for morbidly obese patients, and 25.6 L/min (16%),

25.7 L/min (16%), and 18.9 L/min (21%) for weight loss patients for scenarios 1, 2, and 3, respectively, whereas the observed covariate trend between morbidly obese patients and weight loss patients was identical for the different scenarios. Other model parameters and the goodness-of-fit plots were very similar across the scenarios. These  $Q_H$  scenarios were tested to evaluate the influence of  $Q_H$  on the parameters of the model because there is no consensus yet on the exact changes in  $Q_H$  upon morbid obesity and subsequent weight loss surgery. Although there is no persuasive

**Table 2** Patient characteristics (mean  $\pm$  SD)

	Morbidly obese patients before surgery ( $n = 20$ )	Minimum-maximum	Patients after bariatric surgery ( $n = 18$ of 20)	Minimum-maximum
Female/male	12/8		11/7	
Age, y	43.6 $\pm$ 7.6	26 – 57	45.5 $\pm$ 7.4	27 – 58
Body weight, kg	144.4 $\pm$ 21.7	112 – 186	98.3 $\pm$ 18.0	62 – 138
BMI, kg/m <sup>2</sup>	47.1 $\pm$ 6.5	40 – 68	31.9 $\pm$ 5.9	24 – 50
Weight loss, kg	–	–	44.5 $\pm$ 10.2	21 – 58

BMI, body mass index.

**Table 3** Blood parameter estimates of the final semi-PBPK model including covariates for scenario 1

Parameter	Parameter definition	Value (RSE %)	Bootstrap value (SE)
<b>Midazolam</b>			
$CL_{int,H}$ morbidly obese (L/min)	Intrinsic hepatic clearance morbidly obese	16.8 (14)	16.9 (2.4)
$CL_{int,H}$ weight loss patients (L/min)	Intrinsic hepatic clearance weight loss patients	25.5 (15)	25.4 (4.2)
$CL_{int,G}$ (L/min)	Intrinsic gut wall clearance	0.0199 (35)	0.0207 (0.007)
$K_a$ morbidly obese = $K_{tr}$ ( $\text{min}^{-1}$ )	Oral absorption rate	0.126 (10)	0.126 (0.01)
$K_a$ weight loss patients = $K_{tr}$ ( $\text{min}^{-1}$ )	Oral absorption rate	0.242 (9)	0.241 (0.02)
$V_{central}$ weight loss patients (L)	Central midazolam volume of distribution	66.9 (13)	68.1 (8.7)
$V_{central}$ morbidly obese = $V_{central, 144 \text{ kg}} * (1 + X \text{ (TBW-144)})$			
$V_{central, 144 \text{ kg}}$ (L) = $V_{central}$ weight loss patients	Central midazolam volume of distribution for a 144 kg individual	66.9 (13)	68.1 (8.7)
X	Covariate effect of TBW on $V_{central}$	0.0435 FIX	0.0435 FIX
$V_{peri 1}$ weight loss patients (L)	First peripheral volume of distribution	31.0 (19)	32.0 (6.5)
$V_{peri 1}$ morbidly obese = $V_{peri 1, 144 \text{ kg}} * (\text{TBW}/144)^Y$			
$V_{peri 1, 144 \text{ kg}}$ (L) = $V_{peri 1}$ weight loss patients	First peripheral volume of distribution	31.0 (19)	32.0 (6.5)
Y	Exponent of covariate function	3.93 FIX	3.93 FIX
$V_{peri 2}$ (L) = $V_{peri 1} * Z$	Second peripheral volume of distribution		
Z		10.8 (13)	11.1 (1.7)
$Q_1$ (L/min)	First intercompartmental clearance	1.41 (15)	1.35 (0.2)
$Q_2$ (L/min) = $Q_1 * A$	Second intercompartmental clearance		
A		3.22 FIX	3.22 FIX
<b>1-OH-Midazolam</b>			
$V_{central, 1-OH}$ (L)	Central volume of distribution	41.7 (11)	41.9 (4.7)
$V_{peri, 1-OH}$ (L)	Peripheral volume of distribution	16.4 (25)	17.4 (4.4)
$Q_{1-OH}$ (L/min)	Intercompartmental clearance	0.652 (23)	0.65 (0.15)
$CL_{int,H,1-OH}$ (L/min)	Intrinsic hepatic clearance	27.4 (9)	27.2 (2.6)
$CL_{int,G,1-OH}$ (L/min)	Intrinsic gut wall clearance	11.9 (180)	$4.7 * 10^{22}$ ( $7.3 * 10^{23}$ )
<b>Interindividual variability</b>			
$K_a$ (%)	Oral absorption rate	44 (20)	43 (19)
$V_{central}$ (%)	Central volume of distribution	63 (49)	61 (38)
$V_{peripheral 1}$ (%)	First peripheral volume of distribution	113 (24)	115 (49)
$CL_{int,H}$ (%)	Intrinsic hepatic clearance	48 (21)	47 (20)
$CL_{int,G}$ (%)	Intrinsic gut wall clearance	493 (35)	582 (168)
<b>Residual variability</b>			
Morbidly obese patients (%)		32.6 (18)	32.2 (13)
Weight loss patients (%)		23.7 (8)	23.6 (7)

A, factor difference with morbidly obese patients;  $CL_{int,G}$ , intrinsic gut wall clearance;  $CL_{int,H}$ , intrinsic hepatic clearance; FIX, fixed value;  $K_a$ , oral absorption rate;  $K_{tr}$ , transit compartment rate; Q, intercompartmental clearance; RSE, relative standard error; TBW, total body weight (kg); V, volume of distribution; X, coefficient of covariate relationship; Y, exponent of covariate relationship.

argument for choosing one  $Q_H$  scenario above another, the final parameter estimates and bootstrap results (98% successful) of scenario 1 are presented in **Table 3** and goodness-of-fit plots of this final model are shown in **Figure 2b**.

The different scenarios for hepatic blood flow slightly influenced the calculated values for midazolam plasma clearance,  $F_H$  and  $F_G$ , even though the differences between the morbidly obese patients and weight loss patients remained quite similar per scenario (**Figure 4**). In general, for weight loss patients, higher midazolam plasma clearance (upper row of **Figure 4**, a median increase of 1.28, 1.34, and 1.33, for scenarios 1, 2, and 3, respectively) and lower  $F_H$  (middle row, median decrease of 0.84, 0.83, and 0.88, respectively) was observed.  $F_G$  seems to be close to one for weight loss patients, whereas the morbidly obese patient group exhibits large interindividual variability (lower row of **Figure 4**).

Finally, the influence of weight loss surgery on hepatic CYP3A activity was further explored using the SimCYP simulator.<sup>28</sup> Based on the findings for hepatic intrinsic midazolam clearance of the semi-PBPK model, CYP3A abundances in the liver of the “morbidly obese population” was 1.5 times increased and plasma clearance values for midazolam, cyclosporine, alprazolam, and triazolam were simulated. **Figure 5** shows that this increase in CYP3A abundance resulted in a 1.22 increase of midazolam plasma clearance and a median 1.41, 1.37, and 1.30 increase of plasma clearance for CYP3A substrates cyclosporine, alprazolam, and triazolam, respectively.

## DISCUSSION

In this study, we aimed to characterize the PKs of both midazolam and its primary CYP3A-mediated metabolite

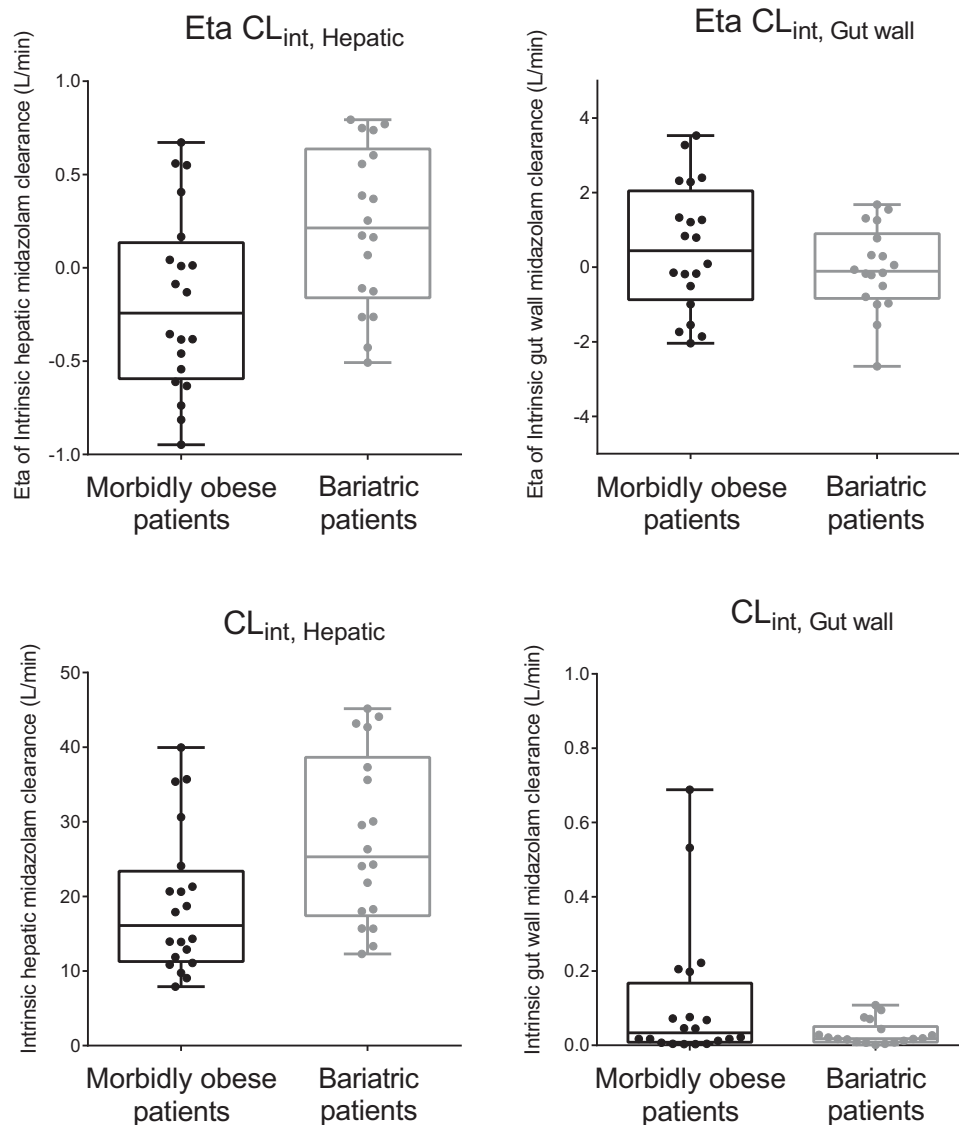


**Figure 3** Box and whisker plots of eta and *post hoc* parameter estimates before addition of covariate effects for intrinsic hepatic ( $CL_{int,H}$ , left panels, shrinkage of 1%) and gut wall ( $CL_{int,G}$ , right panels, shrinkage of 21%) midazolam clearance in morbidly obese patients before (black) and after weight loss surgery (gray).

1-OH-midazolam after oral and i.v. administration in morbidly obese patients before and one year after weight loss surgery, ultimately to evaluate how intrinsic CYP3A activity in the gut wall and liver are affected by weight loss surgery. We found that midazolam and 1-OH-midazolam concentrations could not be described by a regular compartmental model (**Figures 1a** and **2a**) because of presystemic formation of the CYP3A-mediated metabolite 1-OH midazolam for which a semi-PBPK model (**Figures 1b** and **2b**) was needed. Using this model, it was found that midazolam intrinsic hepatic clearance ( $CL_{int,H}$ ) was 1.52 times (95% CI, 1.40–1.64) higher in patients after weight loss surgery, independent of the  $Q_H$  scenario used. In addition, intrinsic midazolam gut wall clearance ( $CL_{int,G}$ ) showed a trend toward lower values in patients after surgery ( $P > 0.05$ ).

Intrinsic hepatic midazolam clearance ( $CL_{int,H}$ ) represents the capacity of the liver to metabolize midazolam into 1-OH-midazolam and therefore represents hepatic CYP3A activity. The estimated  $CL_{int,H}$  for weight loss patients (25.6, 25.7, and 18.9 L/min for scenarios 1, 2, and 3, respectively) was in close agreement with the value reported for healthy volunteers using a very similar semi-PBPK model (27.3; 90% CI, 24.3–30.7 L/min).<sup>14</sup> However, for morbidly obese patients,  $CL_{int,H}$  was lower (16.9, 17.1, and 12.6 L/min for scenarios 1, 2, and 3, respectively), indicating that hepatic CYP3A activity is reduced in morbidly obese patients in comparison to healthy volunteers but normalizes one year after weight loss surgery. Although this recovery of CYP3A activity in the liver upon weight loss surgery has not been reported before, reduced hepatic  $CL_{int}$  because of morbid



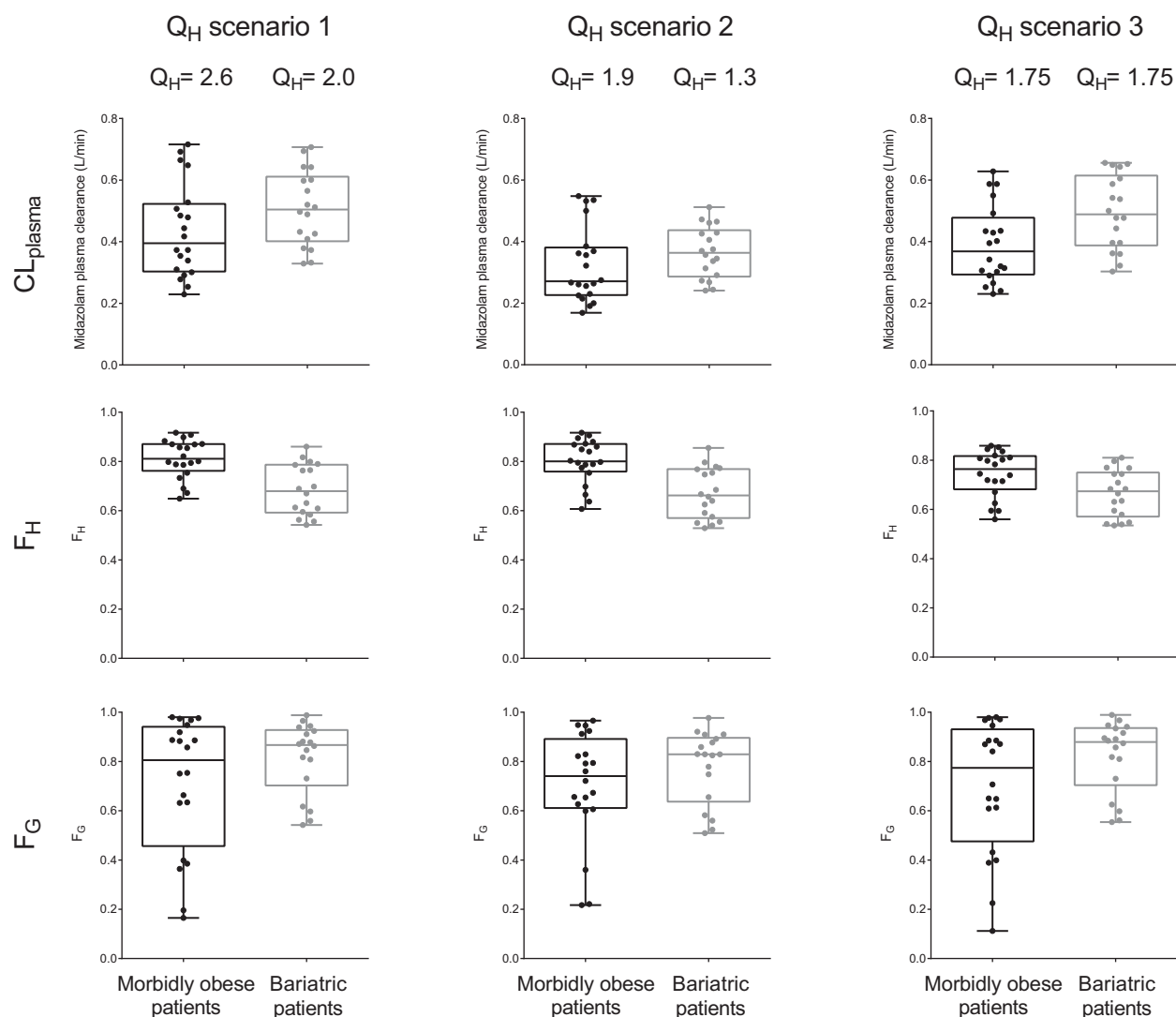


**Figure 4** Box and whisker plots of calculated midazolam plasma clearance (Eq. 7, upper panels),  $F_H$  (Eqs. 1 and 2, middle panels), and  $F_G$  (Eqs. 3 and 5, lower panels) for morbidly obese (black) and weight loss patients (gray) for three different blood flow scenarios ( $Q_H$  in L/min; **Table 1**). Per scenario, the value for hepatic blood flow ( $Q_H$ ) is shown for the median morbidly obese (144 kg) and median weight loss patient (98 kg) of the studied populations.

obesity is supported by *in vitro* studies that show that human liver samples with steatosis exhibit reduced CYP3A activity in comparison to liver samples without steatosis.<sup>30,31</sup> Comparing the observed 1.52 times (range, 1.40–1.64) increase in  $CL_{int,H}$  after a weight loss surgery with values for midazolam plasma clearance from earlier reports on weight loss surgery patients, it seems that this value closely resembles the previously reported 1.7 times increase in midazolam plasma clearance ( $CL_{plasma}$ ).<sup>8,9</sup> However, when calculating midazolam plasma clearance on the basis of midazolam  $CL_{int,H}$  using Eq. 7, we only find a 1.28 increase (scenario 1 and **Figure 4**). In addition, when increasing hepatic CYP3A abundance by 1.5 times in the morbidly obese population of the SimCYP simulator, midazolam plasma clearance only increased 1.22 times. This implies that the increase in midazolam plasma clearance after a weight loss surgery cannot be solely attributed to a

normalization or recovery of hepatic CYP3A activity. Therefore, it may be suggested that another non-CYP3A related process may be involved. This other process may be hepatic blood flow ( $Q_H$ ) or perfusion.<sup>32</sup> In the case of patients after weight loss surgery, potentially an improvement in hepatic microcirculation function (i.e., liver perfusion) because of a reduction in fatty liver may result in a more pronounced increase in midazolam systemic plasma clearance value of 1.7.<sup>33,34</sup> For morbidly obese patients in comparison with nonobese healthy volunteers, the reduced hepatic CYP3A activity (1.52; range, 1.40–1.64; reduced  $CL_{int,H}$ ) found in this analysis may be compensated by an increase in hepatic blood flow in comparison to healthy volunteers resulting in a similar plasma midazolam systemic plasma clearance value compared to healthy volunteers.<sup>16,35</sup> As such, both changes in CYP3A and liver blood flow and/or perfusion contribute to the overall effects

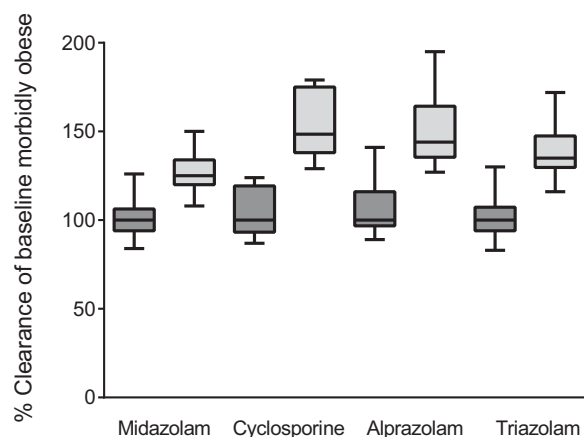


**Figure 5** Box and whisker plots of simulated baseline systemic plasma clearances for the SimCYP morbidly obese patient population (dark gray boxes) and percentage change from baseline when hepatic CYP3a abundance is increased by 1.5 times for the morbidly obese population in the SimCYP simulator (light gray boxes) for four CYP3A substrates.

observed in midazolam plasma clearance in morbidly obese and weight loss patients compared to healthy volunteers.

It seems that information on the hepatic blood flow and perfusion in patients after weight loss surgery is crucial to understand the results and to support the above-described hypothesis that hepatic blood flow or perfusion improves after weight loss surgery. In addition, for morbidly obese patients, information on hepatic blood flow and perfusion is scarce. For this reason, we considered in our analysis different hepatic blood flow scenarios (Table 1, Figure 4), whereas a choice for any of these or other hepatic blood flow scenarios cannot be justified. Scenario 1, in which the hepatic blood flow equation by Brown *et al.*<sup>24</sup> was used, seems to lead to rather large hepatic blood flow values for morbidly obese patients ( $Q_H = 3.7$  L/min at 144 kg). At first sight, scenario 2 seems more plausible for morbidly obese patients, as hepatic blood flow values are derived from the cardiac output function, by the study of Young *et al.*<sup>25</sup> in which data of morbidly obese patients were included, however, the  $Q_H$  values for weight loss patients may be considered too low ( $Q_H = 1.3$  L/min at 98 kg), whereas in healthy volunteers,  $Q_H$  is generally considered to be 1.6 L/min. Scenario 3, assuming a similar blood flow across all body weights, may not be so unrealistic considering the fact that the calculated plasma clearance values are in good agreement with actual results found in our earlier study (Figure 4).<sup>8,9</sup> Future research should elucidate how hepatic blood flow is affected by morbid obesity and weight loss surgery to be able to further improve predictions on how CYP3A-mediated hepatic drug clearance is affected.

Midazolam intrinsic gut wall clearance,  $CL_{int,G}$ , was low in both patient groups in comparison to results from healthy volunteers that were obtained using a similar semi-PBPK model (0.0199 (35%) vs. 0.45 (0.37–0.52) L/min, respectively).<sup>14</sup> As a result, the derived values for  $F_G$  were near one for both patient groups (Figure 4). In addition, a trend for a lower  $CL_{int,G}$  for weight loss patients could be

observed (Figure 3). This result may be attributed to the 75–150 cm bypass of relatively CYP3A rich initial part of the intestines, which is similar to the mechanism that may explain the increase in  $F_G$  for controlled release formulation for highly permeable CYP3A substrates.<sup>36</sup> However, the trend of lower  $CL_{int,G}$  for weight loss patients was not statistically significant. This may be due in part to the high inter-individual variability in  $CL_{int,G}$  observed for both groups. For morbidly obese patients, the relatively low  $CL_{int,G}$  estimate is in line with the increase in midazolam oral bioavailability ( $F_{total}$ ) in comparison to healthy volunteers reported earlier (0.60 (13%) vs. 0.28 (7%);  $P < 0.01$ ).<sup>16</sup>

To further investigate the consequences of 1.52 times (range, 1.40–1.64 times) increased hepatic CYP3A intrinsic clearance for other drugs, the SimCYP simulator was used in which a 1.5 increase in hepatic CYP3A abundance in the morbidly obese population was mimicked. For the CYP3A substrates cyclosporine, alprazolam, and triazolam, plasma clearance was 1.30–1.41 times increased as opposed to 1.22 for midazolam. This difference in impact on plasma clearance between the drugs may be explained by the difference in extraction ratio of the substrates. Midazolam is considered an intermediate extraction ratio drug ( $E_H = \sim 0.4$ ),<sup>21–23</sup> whereas cyclosporine, alprazolam, and triazolam are low extraction ratio drugs ( $E_H = 0.05–0.25$ ).<sup>37–39</sup> From these simulations, it can be concluded that the systemic plasma clearance of low extraction ratio CYP3A substrates is increased by at least 1.3 times after weight loss surgery, whereas, because of the lack of knowledge on how hepatic blood flow is affected by weight loss surgery, no definite conclusions can be drawn for CYP3A substrates with median and higher extraction ratios. Finally, these exploratory extrapolations should be interpreted with caution, as it has been shown that the *in vivo* clearance of CYP3A probes may correlate poorly.<sup>40</sup>

Finally, despite the substantial improvement of the description of both midazolam and 1-OH-midazolam concentrations over time by the semi-PBPK model, the model slightly overpredicted 1-OH-midazolam concentrations after the i.v. dose for patients after weight loss surgery (Figure 2). However, this was not expected to influence any of the conclusions.

We conclude that a semi-PBPK model taking into account both gut wall and liver processes, adequately describes midazolam and CYP3A-mediated 1-OH-midazolam concentrations after both oral and i.v. administration in morbidly obese patients before and after weight loss surgery. Using this model, it was revealed that, in patients one year after weight loss surgery, CYP3A hepatic intrinsic metabolizing capacity is recovered in comparison to morbidly obese patients before weight loss surgery, whereas CYP3A mediated gut wall intrinsic clearance seems to be lower.

**Acknowledgments.** We acknowledge Jantine Brussee, Elke Krelkels, Jeroen Elassaiss-Schaap, and Sebastian Frechen for their input on the modeling process and model code in NONMEM. This study was sponsored by ZonMW (The Netherlands Organisation for Health Research and Development), project number: 836011008. As an associate editor for

CPT:PSP A. R.-H. was not involved in the review or decision process for this paper.

**Conflict of Interest.** The authors declared no conflict of interest.

**Author Contributions.** C.A.J.K., M.J.E.B., P.A.J.V., A.S.D., B.R., E.P.A.D., A.R.-H., and M.D. wrote the manuscript. C.A.J.K., M.J.E.B., A.S.D., B.R., E.P.A.D., A.R.-H., and M.D. designed the research. C.A.J.K., M.J.E.B., P.A.J.V., A.S.D., and E.P.A.D. performed the research. M.J.E.B., P.A.J.V., and A.S.D. analyzed the data. C.A.J.K., M.J.E.B., P.A.J.V., A.R.-H., and M.D. contributed new reagents/analytical tools.

1. Buchwald, H. *et al.* Bariatric surgery: a systematic review and meta-analysis. *JAMA* **292**, 1724–1737 (2004).
2. Buchwald, H. & Oien, D.M. Metabolic/bariatric surgery worldwide 2011. *Obes. Surg.* **23**, 427–436 (2013).
3. Lazzati, A., Guy-Lachuer, R., Delaunay, V., Szwarcencstein, K. & Azoulay, D. Bariatric surgery trends in France: 2005–2011. *Surg. Obes. Relat. Dis.* **10**, 328–334 (2014).
4. Kral, J.G. & Näslund, E. Surgical treatment of obesity. *Nat. Clin. Pract. Endocrinol. Metab.* **3**, 574–583 (2007).
5. Edwards, A. & Ensom, M.H. Pharmacokinetic effects of bariatric surgery. *Ann. Pharmacother.* **46**, 130–136 (2012).
6. Sjöström, L. *et al.* Lifestyle, diabetes, and cardiovascular risk factors 10 years after bariatric surgery. *N. Engl. J. Med.* **351**, 2683–2693 (2004).
7. Brocks, D.R., Ben-Eltriki, M., Gabr, R.Q. & Padwal, R.S. The effects of gastric bypass surgery on drug absorption and pharmacokinetics. *Expert Opin. Drug Metab. Toxicol.* **8**, 1505–1519 (2012).
8. Brill, M.J. *et al.* The pharmacokinetics of the CYP3A substrate midazolam in morbidly obese patients before and one year after bariatric surgery. *Pharm. Res.* **32**, 3927–3936 (2015).
9. Tandra, S., Chalasani, N., Jones, D.R., Mattar, S., Hall, S.D. & Vuppalanchi, R. Pharmacokinetic and pharmacodynamic alterations in the Roux-en-Y gastric bypass recipients. *Ann. Surg.* **258**, 262–269 (2013).
10. Jamei, M. *et al.* Population-based mechanistic prediction of oral drug absorption. *AAPS J.* **11**, 225–237 (2009).
11. Heizmann, P. & Ziegler, W.H. Excretion and metabolism of <sup>14</sup>C-midazolam in humans following oral dosing. *Arzneimittelforschung* **31**, 2220–2223 (1981).
12. Zanger, U.M. & Schwab, M. Cytochrome P450 enzymes in drug metabolism: regulation of gene expression, enzyme activities, and impact of genetic variation. *Pharmacol. Ther.* **138**, 103–141 (2013).
13. Yang, J., Kjellsson, M., Rostami-Hodjegan, A. & Tucker, G.T. The effects of dose staggering on metabolic drug-drug interactions. *Eur. J. Pharm. Sci.* **20**, 223–232 (2003).
14. Frechen, S. *et al.* A semiphenological population pharmacokinetic model for dynamic inhibition of liver and gut wall cytochrome P450 3A by voriconazole. *Clin. Pharmacokinet.* **52**, 763–781 (2013).
15. Flockhart, A. Cytochrome P450 drug interaction table. <<http://www.greenbridgemed.com/wp-content/uploads/2011/09/Drugs-using-P450-Hepatic-metabolism.pdf>>.
16. Brill, M.J. *et al.* Midazolam pharmacokinetics in morbidly obese patients following semi-simultaneous oral and intravenous administration: a comparison with healthy volunteers. *Clin. Pharmacokinet.* **53**, 931–941 (2014).
17. Beal, S., Sheiner, L.B., Boeckmann, A. & Bauer, R.J. NONMEM user's guides (1988–2011) (Ellicott City, MD, 2011).
18. Savic, R.M., Jonker, D.M., Kerbusch, T. & Karlsson, M.O. Implementation of a transit compartment model for describing drug absorption in pharmacokinetic studies. *J. Pharmacokinet. Pharmacodyn.* **34**, 711–726 (2007).
19. Yang, J., Jamei, M., Yeo, K.R., Tucker, G.T. & Rostami-Hodjegan, A. Prediction of intestinal first-pass drug metabolism. *Curr. Drug Metab.* **8**, 676–684 (2007).
20. Yang, J., Jamei, M., Yeo, K.R., Rostami-Hodjegan, A. & Tucker, G.T. Misuse of the well-stirred model of hepatic drug clearance. *Drug Metab. Dispos.* **35**, 501–502 (2007).
21. Thummel, K.E. *et al.* Oral first-pass elimination of midazolam involves both gastrointestinal and hepatic CYP3A-mediated metabolism. *Clin. Pharmacol. Ther.* **59**, 491–502 (1996).
22. Gorski, J.C., Jones, D.R., Haehner-Daniels, B.D., Hamman, M.A., O'Mara, E.M. Jr. & Hall, S.D. The contribution of intestinal and hepatic CYP3A to the interaction between midazolam and clarithromycin. *Clin. Pharmacol. Ther.* **64**, 133–143 (1998).
23. Lee, J.I., Chaves-Gnecco, D., Amico, J.A., Kroboth, P.D., Wilson, J.W. & Frye, R.F. Application of semisimultaneous midazolam administration for hepatic and intestinal cytochrome P450 3A phenotyping. *Clin. Pharmacol. Ther.* **72**, 718–728 (2002).
24. Brown, R.P., Delp, M.D., Lindstedt, S.L., Rhomberg, L.R. & Bellies, R.P. Physiological parameter values for physiologically based pharmacokinetic models. *Toxicol. Ind. Health* **13**, 407–484 (1997).
25. Young, J.F. *et al.* Human organ/tissue growth algorithms that include obese individuals and black/white population organ weight similarities from autopsy data. *J. Toxicol. Environ. Health A* **72**, 527–540 (2009).
26. Williams, L.R. & Leggett, R.W. Reference values for resting blood flow to organs of man. *Clin. Phys. Physiol. Meas.* **10**, 187–217 (1989).
27. Keizer, R.J. *et al.* Incorporation of concentration data below the limit of quantification in population pharmacokinetic analyses. *Pharmacol. Res. Perspect.* **3**, e00131 (2015).
28. Jamei, M., Marciniak, S., Feng, K., Barnett, A., Tucker, G. & Rostami-Hodjegan, A. The Simcyp population-based ADME simulator. *Expert Opin. Drug Metab. Toxicol.* **5**, 211–223 (2009).
29. Ghobadi, C. *et al.* Application of a systems approach to the bottom-up assessment of pharmacokinetics in obese patients: expected variations in clearance. *Clin. Pharmacokinet.* **50**, 809–822 (2011).
30. Fisher, C.D. *et al.* Hepatic cytochrome P450 enzyme alterations in humans with progressive stages of nonalcoholic fatty liver disease. *Drug Metab. Dispos.* **37**, 2087–2094 (2009).
31. Kolwankar, D. *et al.* Association between nonalcoholic hepatic steatosis and hepatic cytochrome P-450 3A activity. *Clin. Gastroenterol. Hepatol.* **5**, 388–393 (2007).
32. Alexander, J.K., Dennis, E.W., Smith, W.G., Amad, K.H., Duncan, W.C. & Austin, R.C. Blood volume, cardiac output, and distribution of systemic blood flow in extreme obesity. *Cardiovasc. Res. Cent. Bull.* **1**, 39–44 (1962–1963).
33. Ijaz, S., Yang, W., Winslet, M.C. & Seifalian, A.M. Impairment of hepatic microcirculation in fatty liver. *Microcirculation* **10**, 447–456 (2003).
34. Lassailly, G. *et al.* Bariatric surgery reduces features of nonalcoholic steatohepatitis in morbidly obese patients. *Gastroenterology* **149**, 379–388; quiz e15–e16 (2015).
35. Greenblatt, D.J., Abernethy, D.R., Locniskar, A., Harmatz, J.S., Limjuco, R.A. & Shader, R.I. Effect of age, gender, and obesity on midazolam kinetics. *Anesthesiology* **61**, 27–35 (1984).
36. Olivares-Morales, A., Kamiyama, Y., Darwich, A.S., Aarons, L. & Rostami-Hodjegan, A. Analysis of the impact of controlled release formulations on oral drug absorption, gut wall metabolism and relative bioavailability of CYP3A substrates using a physiologically-based pharmacokinetic model. *Eur. J. Pharm. Sci.* **67**, 32–44 (2015).
37. Venkataramanan, R., Ptachcinski, R.J., Burckart, G.J., Yang, S. & Starzl, T.E. Extraction ratio of cyclosporine in a liver transplant patient with organ rejection. *J. Pharm. Sci.* **74**, 901–902 (1985).
38. Ohtsuka, T. *et al.* Alprazolam as an in vivo probe for studying induction of CYP3A in cynomolgus monkeys. *Drug Metab. Dispos.* **38**, 1806–1813 (2010).
39. Kroboth, P.D., McAuley, J.W., Kroboth, F.J., Bertz, R.J. & Smith, R.B. Triazolam pharmacokinetics after intravenous, oral, and sublingual administration. *J. Clin. Psychopharmacol.* **15**, 259–262 (1995).
40. Masica, A.L., Mayo, G. & Wilkinson, G.R. In vivo comparisons of constitutive cytochrome P450 3A activity assessed by alprazolam, triazolam, and midazolam. *Clin. Pharmacol. Ther.* **76**, 341–349 (2004).
41. Ito, K., Ogihara, K., Kanamitsu, S. & Itoh, T. Prediction of the in vivo interaction between midazolam and macrolides based on in vitro studies using human liver microsomes. *Drug Metab. Dispos.* **31**, 945–954 (2003).
42. Mandema, J.W., Tuk, B., van Steveninck, A.L., Breimer, D.D., Cohen, A.F. & Danhof, M. Pharmacokinetic-pharmacodynamic modeling of the central nervous system effects of midazolam and its main metabolite alpha-hydroxymidazolam in healthy volunteers. *Clin. Pharmacol. Ther.* **51**, 715–728 (1992).

© 2015 The Authors CPT: Pharmacometrics & Systems Pharmacology published by Wiley Periodicals, Inc. on behalf of American Society for Clinical Pharmacology and Therapeutics. This is an open access article under the terms of the Creative Commons Attribution NonCommercial License, which permits use, distribution and reproduction in any medium, provided the original work is properly cited and is not used for commercial purposes.

Supplementary information accompanies this paper on the CPT: Pharmacometrics & Systems Pharmacology website (<http://www.wileyonlinelibrary.com/psp4>)